

Toggleable transparency states in thermally-shifted multiMRR cascaded filters

*Original*

Toggleable transparency states in thermally-shifted multiMRR cascaded filters / Tunesi, L., Awad, H., Carena, A., Curri, V., Bardella, P.. - ELETTRONICO. - 13371:(2025), pp. 1-5. (SPIE Photonics West - OPTO San Francisco (USA) 28-30 January 2025) [10.1117/12.3044329].

*Availability:*

This version is available at: 11583/2999645 since: 2025-04-29T11:54:52Z

*Publisher:*

SPIE

*Published*

DOI:10.1117/12.3044329

*Terms of use:*

This article is made available under terms and conditions as specified in the corresponding bibliographic description in the repository

*Publisher copyright*

SPIE postprint/Author's Accepted Manuscript e/o postprint versione editoriale/Version of Record con

Copyright 2025 Society of PhotoOptical Instrumentation Engineers (SPIE). One print or electronic copy may be made for personal use only. Systematic reproduction and distribution, duplication of any material in this publication for a fee or for commercial purposes, and modification of the contents of the publication are prohibited.

(Article begins on next page)

# Toggleable transparency states in thermally-shifted multi-MRR cascaded filters

Lorenzo Tunesi<sup>a</sup>, Hasan Awad<sup>a</sup>, Andrea Carena<sup>a</sup>, Vittorio Curri<sup>a</sup>, and Paolo Bardella<sup>a</sup>

<sup>a</sup>Department of electronics and telecommunications, Politecnico di Torino, Turin, Italy

## ABSTRACT

We showcase and analyze a control scheme to leverage thermal-induced transparency in cascaded multistage microring resonator (MRR) structures. MRRs are one of the basic building blocks in integrated photonics, typically used to implement high Q-factor filters and frequency-dependent circuits. While traditionally single-order rings are reserved for straightforward and simple applications, higher-order cascaded structures can be arranged to introduce and implement advanced filters, showcasing larger flat-top bandwidth and allowing precise tailoring of the response. Thermally induced phase delay between the MRRs can be used to achieve precise control of the response, while also allowing a transparent switching state obtained through destructive interference of the different ring responses. In our work, we investigate how this effect can be leveraged to turn off the filtering structure, introducing a toggleable state, while validating the theoretical uses and limitations of the control scheme by implementing the structure through programmable integrated photonic circuits.

**Keywords:** Microring Resonators. Photonic Integrated Circuits. Integrated Switching. Photonic Filters.

## 1. INTRODUCTION

MicroRing Resonators (MRRs) are versatile components that have been implemented in Photonic Integrated Circuits (PICs) for a wide variety of fields. They represent one of the fundamental solutions for filter synthesis and in general for all wavelength-specific applications, such as optical signal processing, neuromorphic, and switching, and have been thoroughly investigated over the years.<sup>1</sup>

In their straightforward configurations, MRRs can be used as first-order elements, coupled to a single or multiple waveguides, to provide basic periodic filtering as simple add-drop elements, although their performance is typically not optimal as high Q-factor filters. Through higher order MRRs implementations, such as cascaded or designed in multistage structures, more advanced filters can be implemented, with better control of extinction ratio, crosstalk, roll-off, and all other main filter parameters.<sup>2</sup>

Although advantageous, these more advanced filter topologies require tuning mechanisms, able to insure compensation of the manufacturing uncertainty, as to tune the different rings to their desired resonance condition. At the same time, active control of the rings, such as thermally,<sup>3</sup> can also allow dynamic tuning of the filter response, altering the central frequency, bandwidth, and spectral properties. In this work we consider such mechanism in a four MRRs structure, arranged in a two-stage second-order ladder topology, highlighting how asymmetric ring tuning can introduce destructive resonance throughout the whole device, leading to a transparent "off" state, traditionally not available in simpler topologies.

This mechanism and topology has also been tested on the Ipronics Smartlight programmable photonic processor,<sup>4</sup> validating the simulation model and design principle.

---

Further author information: (Send correspondence to Lorenzo Tunesi)

Lorenzo Tunesi: E-mail: lorenzo.tunesi@polito.it

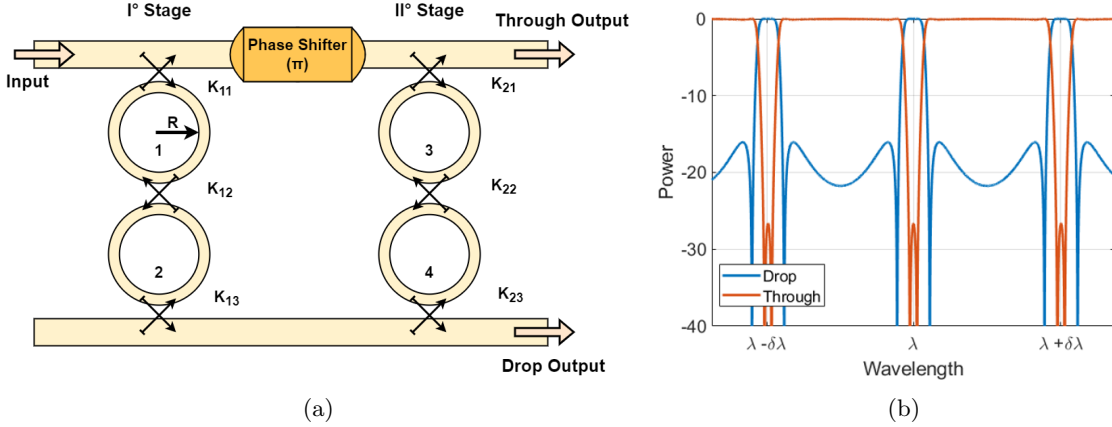


Figure 1: (a) Two-stage Ladder MRR filter. (b) Output response of the Add-Drop element.

## 2. MRR LADDER FILTERS AND TUNING SCHEME

The investigated structure is a four-ring filter arranged in a second order, two-stage, ladder configuration Fig. 1a: the two coupled rings stages are connected through two waveguides, which must be designed to introduce a phase change  $\pi$  between the through and drop output of the first stage.<sup>5</sup>

Higher order structures can be used to further increase the degrees of freedom in the filter design, albeit with diminishing returns, due to the increase in complexity, footprint, and loss.

In the investigated configuration the filter response can be therefore evaluated based on the fundamental MRR length (considered equal in all four rings) and the inter-waveguide and inter-ring coupling coefficients of the two stages, which shape the response. Asymmetry between the rings could be intentionally introduced, although for the target application as flat-top add-drop filter this does not provide any benefit.

Assuming C-band operating range, the MRR radius is set to  $R = 15 \mu\text{m}$  (considering standard Si/SiO<sub>2</sub> integrated platform) with resulting values of the couplings  $\kappa_{11} = \kappa_{13} = 0.8$ ,  $\kappa_{12} = 0.1$ ,  $\kappa_{21} = \kappa_{23} = 0.3$ ,  $\kappa_{22} = 0.2$ . These values lead to the response depicted in Fig. 1b, which showcases an extinction ratio of 30 dB, with a flat-top, high roll-off central channel response. The response of the device has been simulated through the use of Synopsys Optsim suite, which allows the representation of the internal elements, such as waveguides, couplers, and phase shifters, through a circuit-like model. As stated before, these devices require active MRR calibration due to their sensitivity to manufacturing uncertainty, as such we consider each ring to be independently tunable, which has been modeled in our equivalent circuit as a controllable phase-shift in each MRR (Fig. 2a). Even though uncertainty-aware design techniques,<sup>6</sup> or data-driven models<sup>7</sup> can be deployed to compensate the asymmetry

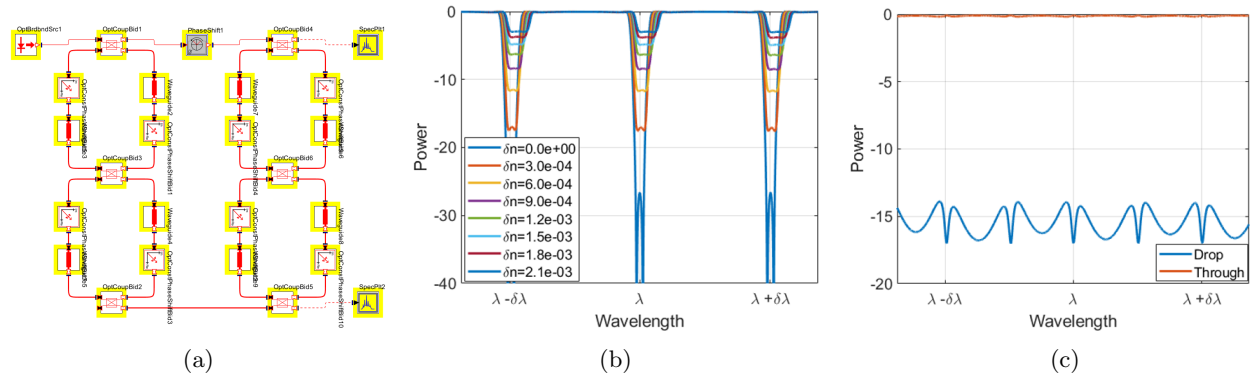


Figure 2: (a) Optsim Circuit Model, showing the circuit representation of the main functional blocks of the device. Frequency response shift for (b) asymmetric index modulation (even-odd rings). (c) Output spectrum for the transparent toggled state.

present in manufactured devices, the MRR control would still be needed for the finer alignment, as well as to maintain dynamic tuning. Dynamic control is traditionally achieved through integrated micro-heaters, although in this work the effect is modeled as a generic phase shift, as to maintain generality toward any form of effective index modulation (thermal, electrical, mechanical, etc.).

While uniform phase shift of all MRRs leads to a simple drift in the channel central wavelength, we can instead observe the proposed transparent state when asymmetric control is applied to the stages: this consists of introducing a phase shift in either the first and fourth rings, or the second and third. The mechanism behind this tuning scheme can be explained by destructive interference, as the asymmetric tuning of the rings compensates the phase shift between the resonant signal coupled to the rings and the one propagating through, switching off the resonance of the device. As the phase shifts tend toward  $\Delta\phi = \pi$  the response at the through port, depicted in Fig. 2b start to flatten. When the exact value  $\Delta\phi = \pi$  is reached the device through response shows almost no wavelength-dependent resonant effects, while only crosstalk ( $-15$  dB) reaches the drop port, with no channel formation, as seen in Fig. 2c.

### 3. EXPERIMENTAL VALIDATION

In order to test this transparent state, the two-stage device was implemented in the iPronics Smartlight programmable optical processor. The Smartlight is composed of a hexagonal mesh of Mach-Zehnder Interferometers (MZIs),<sup>8</sup> which can be programmed as cross-bar switches, adjustable couplers, and delay lines, which are the functional blocks required to implement the filter.

The programmed mesh structure can be seen in Fig. 3a, with each rectangle representing an independent MZI: the orange colored elements are tuned in the BAR state, the black represents a CROSS state, and the green custom coupling, while the gray ones are inactive.

The experiment uses an Erbium ASE source (HP 83438A) which is amplified through an EDFA (Optigain Inc. 2000) and sent through the programmed mesh after polarization alignment. The external ports of the mesh are each connected to an independent fiber, which can be used bidirectionally to both insert the signal and/or measure the output. Although the Smartlight is equipped with an internal wave analyzer, the measurements have been carried out through an external one (Finisar 1500S), which has higher resolution and bandwidth.

The measurements were taken for the default state (On), after calibration and alignment of the four MRRs, and for the proposed transparent state (Off), changing the MZI cells in the first and fourth ring to introduce the additional phase shift. The results are shown for the drop and through ports in Fig. 3b and Fig. 3c respectively. The first major difference is represented by the channel width and periodicity, which is due to the much larger ring size in the programmable mesh. Due to the fact that the basic MZI cell is around  $L \approx 900 \mu\text{m}$  and a single MRR needs six cells, the equivalent radius is around  $R \approx 850 \mu\text{m}$ . This, however, should not affect the overall response shape, which is instead different even in the default "On" case: due to the length of the MZIs the

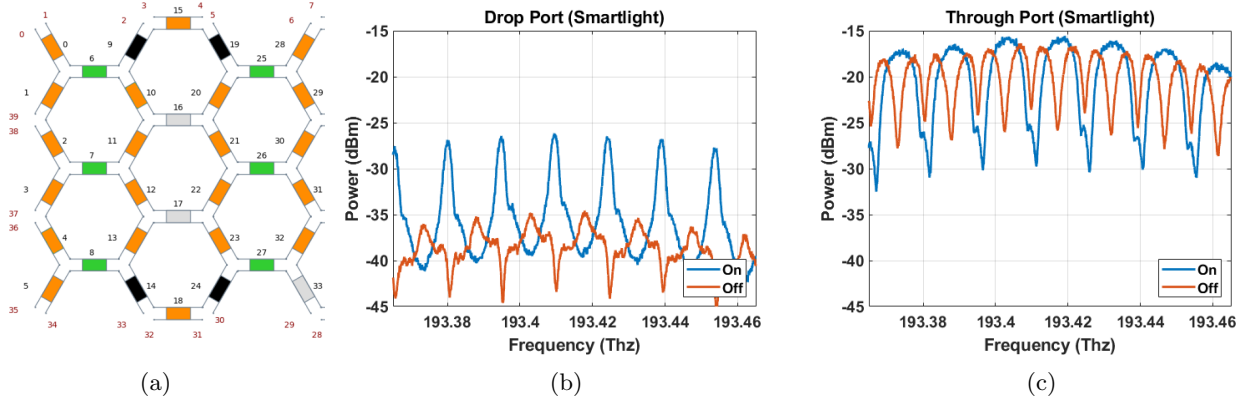


Figure 3: (a) Programmed circuit on the Smartlight photonic processor. Measured frequency response on the Smartlight programmed circuit depicting the response in the default and the toggled state for (b) the drop port and (c) the through port.

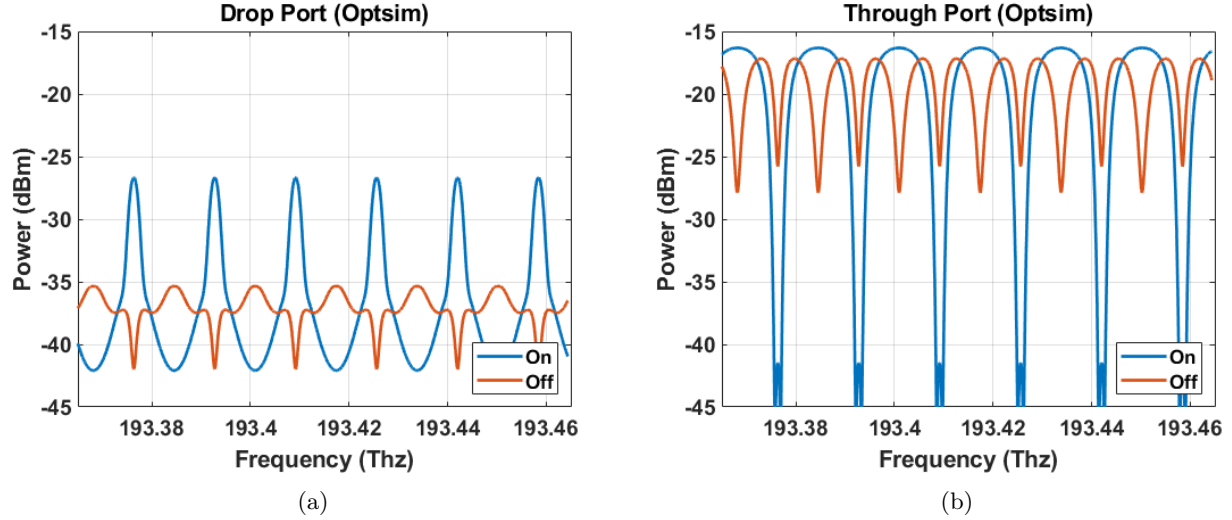


Figure 4: Simulated response of the fitted Optsim circuit depicting the response in the default and the toggled state for the drop port (a) and the through port (b).

propagation losses are much higher than the ones originally simulated. Without considering the fiber-to-chip losses of the Smartlight, which do not affect the resonance of the MRR, the MZIs still exhibit high losses (0.5 dB) that deeply affect the drop response. Similarly in the transparent state the responses are quite different from the original results, with a clear attenuation of the resonant channel in the drop port (Fig. 3b), albeit still high overall losses in the through response (Fig. 3c). This can be once again explained by the asymmetric losses experienced by the signal during the propagation in the ladder device: even though the resonance is suppressed, no recombination happens at the through port, as the majority of the signal is dissipated through the MRRs. This explanation can be easily tested by fitting the Optsim model blocks with similar propagation characteristics to the Smartlight MZIs. As shown in Fig. 4a and Fig. 4b, the simulation matches the experimental results quite closely, showcasing how the mechanism still works in minimizing the channel resonance, albeit with high propagation loss no meaningful transparent state can be seen at the through port.

While the losses in the Smartlight processor cannot be changed, the results show that the correct resonance alignment to toggle the transparent state can be reached through thermo-optic calibration setups. Furthermore

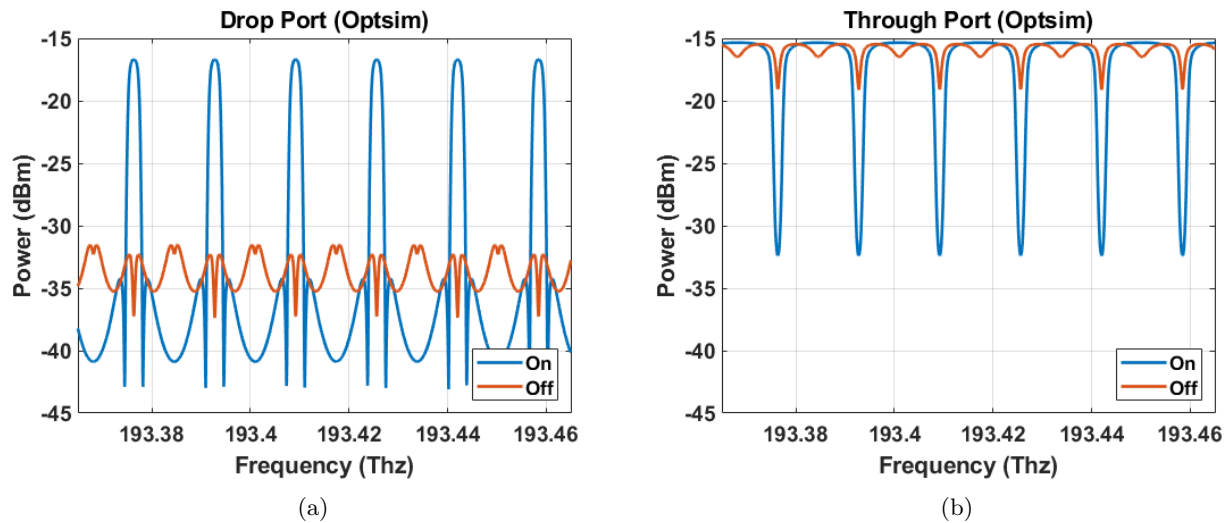


Figure 5: Simulated response of the low-loss Optsim circuit depicting the response in the default and the toggled state for the drop port (a) and the through port (b).

by considering integration into any low-loss Silicon Photonics platform,<sup>9</sup> and through optimized design of the MRRs,<sup>10</sup> the roundtrip losses can be reduced dramatically. As depicted in Fig. 5, with more reasonable losses, even for large equivalent MRRs ( $R \approx 850 \mu\text{m}$ ), the response resemble the original behavior, with a clear attenuation of the resonance effect, and extra losses in the range  $IL \approx -3 \text{ dB}$  instead of the measured  $IL \approx -12 \text{ dB}$ .

#### 4. CONCLUSIONS

We have showcased an experimental implementation of a two-stage ladder MRR filter, highlighting the response when selective index control is applied to the MRRs to cancel out the resonant effects. This transparent toggleable state is shown to be severely affected by the insertion and propagation losses of the Smartlight processor used to implement the device. The model has been fitted to account for such experimental losses, showing that the MRR alignment can be correctly reproduced, albeit less effective due to the hardware limitations.

Low-loss integrated implementation is shown through simulation to potentially yield the theoretical behavior, especially considering smaller MRRs size with respect to the experimental ones, whose minimum size is limited by the programmable cells in the Smartlight optical processor.

#### ACKNOWLEDGMENTS

The authors thank Professor Francesco Da Ros, his team, and DTU, for the support in the experimental activity described in this manuscript.

#### REFERENCES

- [1] Van, V., [*Optical microring resonators: theory, techniques, and applications*], CRC Press (2016).
- [2] Peng, Z., Komatsubara, T., Yamauchi, M., and Arakawa, T., “Design of a series-coupled microring resonator wavelength filter using the digital filter design method,” *J. Opt. Soc. Am. B* **38**, 2837–2846 (Oct 2021).
- [3] Jayatilleka, H., Murray, K., Ángel Guillén-Torres, M., Caverley, M., Hu, R., Jaeger, N. A. F., Chrostowski, L., and Shekhar, S., “Wavelength tuning and stabilization of microring-based filters using silicon in-resonator photoconductive heaters,” *Opt. Express* **23**, 25084–25097 (Sep 2015).
- [4] iPrronics. <https://ipronics.com/>.
- [5] Masilamani, A. P. and Van, V., “Design and realization of a two-stage microring ladder filter in silicon-on-insulator,” *Opt. Express* **20**, 24708–24713 (Oct 2012).
- [6] Shafiee, A., Mirza, A., Sunny, F., Banerjee, S., Chakrabarty, K., Pasricha, S., and Nikdast, M., “Inexact silicon photonics,” in [*Photonics in Switching and Computing*], (2021).
- [7] Tunesi, L., Khan, I., Masood, M. U., Marchisio, A., Ghillino, E., Curri, V., Carena, A., and Bardella, P., “Machine learning aided prediction of fabrication uncertainties in integrated multi-ring filters,” in [*CLEO 2023*], *CLEO 2023*, STh4H.2, Optica Publishing Group (2023).
- [8] Pérez, D., Gasulla, I., Capmany, J., and Soref, R. A., “Reconfigurable lattice mesh designs for programmable photonic processors,” *Opt. Express* **24**, 12093–12106 (May 2016).
- [9] Heck, M. J. R., Bauters, J. F., Davenport, M. L., Spencer, D. T., and Bowers, J. E., “Ultra-low loss waveguide platform and its integration with silicon photonics,” *Laser & Photonics Reviews* **8**(5), 667–686 (2014).
- [10] Puckett, M. W., Wang, J., Bose, D., Brodnik, G. M., Wu, J., Nelson, K., and Blumenthal, D. J., “Silicon nitride ring resonators with 0.123 db/m loss and q-factors of 216 million for nonlinear optical applications,” in [*2019 Conference on Lasers and Electro-Optics Europe European Quantum Electronics Conference (CLEO/Europe-EQEC)*], 1–1 (2019).